AUTHOR QUERY FORM

ELSEVIER	Journal: COGE Article Number: 1322	Please e-mail or fax your responses and any corrections to: E-mail: corrections.esil@elsevier.sps.co.in Fax: +31 2048 52799

Dear Author,

Any queries or remarks that have arisen during the processing of your manuscript are listed below and highlighted by flags in the proof. Please check your proof carefully and mark all corrections at the appropriate place in the proof (e.g., by using on-screen annotation in the PDF file) or compile them in a separate list.

For correction or revision of any artwork, please consult http://www.elsevier.com/artworkinstructions.

Articles in Special Issues: Please ensure that the words 'this issue' are added (in the list and text) to any references to other articles in this Special Issue.

Uncited references: References that occur in the reference list but not in the text – please position each reference in the text or delete it from the list.

Missing references: References listed below were noted in the text but are missing from the reference list – please make the list complete or remove the references from the text.

Location in article	Query / remark Please insert your reply or correction at the corresponding line in the proof
Q1	Please note that Table 4 has been changed to Table 5. Kindly check.

Electronic file usage

Sometimes we are unable to process the electronic file of your article and/or artwork. If this is the case, we have proceeded by:

☐ Scanning (parts of) your article ☐ Rekeying (parts of) your article ☐ Scanning the artwork

Thank you for your assistance.

Computers and Geotechnics xxx (2010) xxx–xxx

Contents lists available at ScienceDirect

Computers and Geotechnics

journal homepage: www.elsevier.com/locate/compgeo

Probabilistic analysis of the inverse analysis of an excavation problem

J. Baroth, Y. Malecot *

Université Joseph Fourier – Grenoble I, Laboratoire Sols Solides Structures – Risques, CNRS UMR 5521, BP 53, 38041 Grenoble Cedex 9, France

ARTICLE INFO

Article history:
Received 2 September 2008
Received in revised form 12 December 2009
Accepted 29 December 2009
Available online xxxx

Keywords:
Prediction
Inverse analysis
Genetic algorithm
Stochastic finite element method
Excavation
Sheetpile wall field test

ABSTRACT

This study presents the probabilistic analysis of the inverse analysis of an excavation problem. Two techniques are used during two successive stages. First, a genetic algorithm inverse analysis is conducted to identify soil parameters from *in situ* measurements (i.e. first stage of the construction project). For a given tolerable error between the measurement and the response of the numerical model the genetic algorithm is able to generate a statistical set of soil parameters, which may then serve as input data to a stochastic finite element method. The second analysis allows predicting a confidence interval for the final behaviour of the geotechnical structure (i.e. second stage of the project). The tools employed in this study have already been presented in previous papers, but the originality herein consists of coupling them. To illustrate this method, a synthetic excavation problem with a very simple geometry is used.

1. Introduction

In civil engineering, the well-known finite element method (FEM) allows an accurate representation of structures. Yet, many sources of uncertainty unfortunately still exist (e.g. material, geometry, solicitation). Geotechnical problems are particularly affected by poor knowledge of soil behaviour. The inherent heterogeneity and complexity of soil behaviour yield a model of geotechnical structures that inevitably proves both uncertain and simplified.

This high uncertainty of soil knowledge has led to a successful experience with the observational method for designing geotechnical structures. Developed by Terzaghi and Peck [1,2], observational approaches are nowadays recommended within the European design code [3], which promotes their use given that the evolution of geotechnical behaviour for a building cannot be easily predicted.

Moreover, thanks to the availability of numerical tools, the identification of constitutive parameters by means of inverse analysis [4] has become a timely topic of growing importance in the geotechnical field [5–13]. However, most methods cited in the literature for solving the inverse problem in geotechnical engineering assume uniqueness of the solution and do not take into account modelling errors or *in situ* measurement uncertainties. This uncertainty implies that a unique exact solution to the inverse problem in fact does not exist, but instead an infinite number of approximated solutions can be found. Recently, Levasseur et al. developed an inverse analysis (IA) method based on a genetic algorithm (GA) that enables identifying a representative set of these approximated solutions [14–16]. In using the same techniques, this paper presents a probabilistic analysis of this IA method, applied to an excavation problem, in order to identify a confidence interval for the final behaviour of the geotechnical structure.

To begin, a genetic algorithm inverse analysis will be introduced for the purpose of identifying soil parameters from *in situ* measurements (i.e. first stage of the construction project). For a given tolerable error between the measurements and the response of the numerical model, the genetic algorithm is able to determine a statistical set of soil parameters (Section 2), making the assumption that measurements have been done in a homogeneous stratum. It is then assumed that identified parameters can be modelled as random variables. These identified parameters will then serve as input data to a stochastic finite element method (SFEM) [17] (Section 3). SFEMs [18,19] have undergone modifications over the past several decades to overcome the problem of uncertainty propagation through a finite element model, as opposed to Monte Carlo simulations [20]. The recent method [17] has already been applied in structural engineering problems [21,22] and allows predicting a confidence interval for the final geotechnical structure behaviour (i.e. second stage of the project).

To illustrate this method, principles of the proposed approach is summarized in Fig. 1. A synthetic excavation problem will then be modelled using a commercial finite element code (Section 4). The horizontal displacements of a diaphragm wall subsequent to the

* Corresponding author. Tel.: +33 4 76 82 70 44; fax: +33 4 76 82 44 43.
E-mail address: Yann.Malecot@ujf-grenoble.fr (Y. Malecot).

0266-352X/$ - see front matter © 2010 Elsevier Ltd. All rights reserved.
doi:10.1016/j.compgeo.2009.12.006

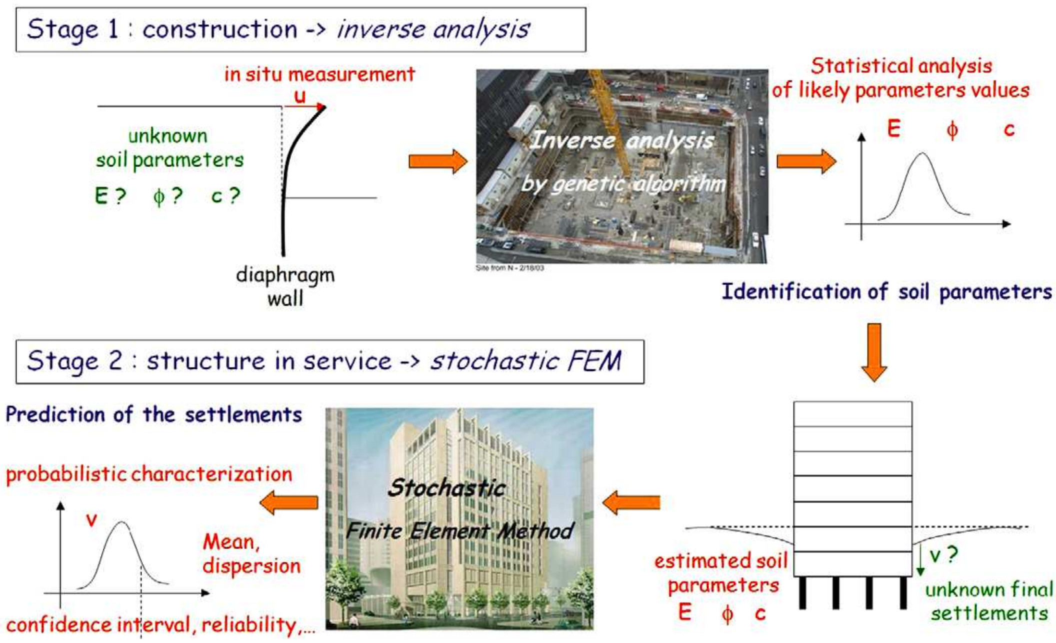

Fig. 1. Principle of the proposed method combining an inverse analysis and a probabilistic approach.

first excavation stage will be used as *in situ* measurements for the identification process. Lastly, a confidence interval for wall displacements of the structure while in service will be estimated.

2. The genetic algorithm (GA) inverse analysis

For this first part of the study, we have assumed a given level of tolerable error between the measurement and the response of the numerical model. Next, a genetic algorithm (GA) optimisation process is implemented to identify all solutions to the inverse problem (Fig. 2). This method is known to be robust and efficient in its ability to solve very complex problems [23]. Its application to the geotechnical field has already been presented in Levasseur et al. [15], and the method has been shown to yield the best solution to an inverse problem even with a flat or noisy error function. In the case of solution non-uniqueness, a representative sample of inverse problem solutions can indeed be identified [16,17].

2.1. Error function

The discrepancy between experimental behaviour and modelled behaviour is expressed as a scalar error function, F_{err}, as intended in the least squares method introduced by Levasseur et al. [15]:

$$F_{err} = \left(\frac{1}{M} \sum_{i=1}^{M} \frac{(Ue_i - Un_i)^2}{\Delta U_i^2} \right)^{1/2} \tag{1}$$

where M is the number of measurement points, Ue_i the ith experimental measured value, Un_i the corresponding value of the numerical calculation, and $1/\Delta U_i$ the weight of the discrepancy between Ue_i and Un_i. ΔU_i represents the experimental (and/or numerical) uncertainty of the ith measurement point. This error function corresponds to the objective function commonly found in the literature [24]. A tolerable error δF_{err} on this error function could eventually be expressed in percentage terms [15].

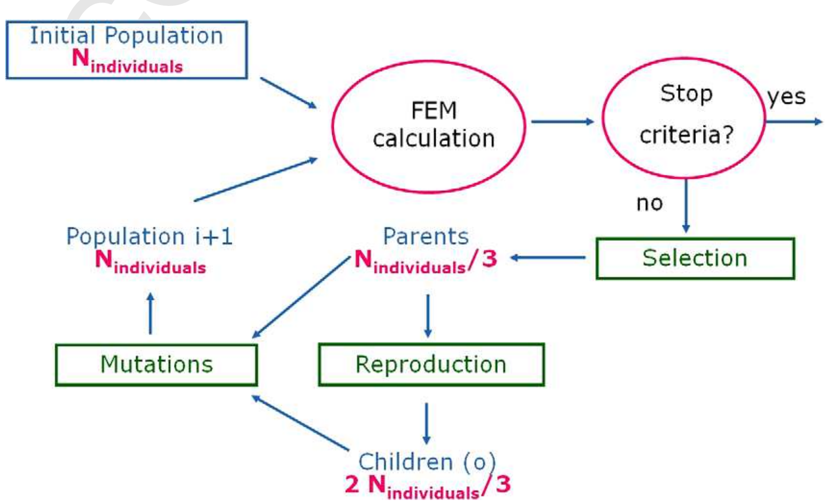

Fig. 2. Principle of the genetic algorithm inverse analysis procedure.

Please cite this article in press as: Baroth J, Malecot Y. Probabilistic analysis of the inverse analysis of an excavation problem. Comput Geotech (2010), doi:10.1016/j.compgeo.2009.12.006

2.2. Genetic algorithm

To minimize this error function, the genetic algorithm method is employed. Genetic algorithms have been inspired by Darwin's theory of evolution. The basic outline of the algorithm, as developed by Levasseur et al. [15] and summarized below, has been derived from the studies conducted by Goldberg [23] and Renders [25].

Since the error function $F_{err}(y)$ is defined as a scalar for each set of N_p uncertain parameters, noted as a vector y, the inverse problem is "solved" as a minimization problem in an N_p-dimension space restricted to authorised values of y between $y_{\min}$ and $y_{\max}$. The key stages of this algorithm are as follows:

2.2.1. Encoding, both individual and population

We begin by defining y as an individual and then each component of y as a gene. Each gene is binary-encoded and concatenated to the other components with a given number of bytes, N_b. The choice of this number is directly correlated with the expected precision of the parameter value. The concatenation of several genes forms an individual, with each individual serving to define a point of the search space.

2.2.2. Generation of an initial population

A group of N_I individuals is randomly chosen within the search space. The scalar error function for each individual of a population is then evaluated. The mechanisms of selection, reproduction and mutation are used to induce the population to evolve towards the best individuals in the search space.

2.2.3. Selection

Depending on their fitness (determined from the minimum cost of the scalar error function), only the best $N_I/3$ individuals are preserved when constituting the next population: these are called parents. This "elitist" selection process is known to be more efficient for unimodal function optimisations [23].

2.2.4. Reproduction and crossing

The parents are randomly selected by pairs and crossed over into N_{coup} points in order to generate new offspring pairs. To improve algorithm efficiency, the number N_{coup} is set equal to the number of sought parameters, as proposed by Pal et al. [26]. The crossing process is then repeated until $2N_I/3$ offspring have been created; these new offspring are called children.

2.2.5. Mutation and generation of a new population

Combining parents and children serves to create a new population of N_I individuals. To limit convergence problems while diversifying the population, some new offspring are randomly mutated (inversion of one bit from one gene), with a given mutation probability P_M. The error function of each new individual is then evaluated.

2.2.6. Convergence test

These various stages are repeated until some convergence conditions have been satisfied, i.e. either that the average error function on the parents' part of the population is less than a given error, or that its standard deviation becomes too small. This convergence criterion depends on the quality of both experimental data and problem modelling. For this initial research effort, we have chosen to use synthetic data instead of experimental data.

Once a set of N_S solutions has been identified by the genetic algorithm, a statistical analysis is employed to estimate a mean $\hat{\mu}$ and a covariance matrix $\hat{C}$.

3. Stochastic finite element method (SFEM) prediction

The targeted soil parameters, as characterised by their mean $\hat{\mu}$ and covariance $\hat{C}$, are used as input data to a stochastic finite element method (SFEM) so as to predict a confidence interval for the displacements of the structure in service. Uncertain soil parameters are modelled by a vectorial random variable (r.v.), denoted Y, with a lognormal probability density function (PDF), denoted p_Y, and with mean μ_Y and covariance C_Y (set equal to $\hat{\mu}$ and $\hat{C}$, respectively). For the sake of simplicity, we present the case of a scalar r.v., lognormal Y and we introduce the function T binding Y and X (Gaussian normalisation [17]). This method's main steps [17] are presented below.

1. The first step in this approach consists of rewriting the problem in terms of standardised Gaussian r.v., denoted X (i.e. with a mean of 0 and standard deviation of 1). In the following, r.v. $Z = f(Y)$, which models the mechanical response (displacements), is written as the composite function $f \circ T$ of the r.v. X, such that:

$$Z = f \circ T(X) = g(X) \tag{2}$$

2. The approximation of the function g is a projection onto the truncated basis $\{L_i\}_{i=1,\ldots,n}$

$$g(X) \approx \tilde{g}(X) = \sum_{i=1}^{n} \alpha_i \cdot \prod_{\substack{k=1 \\ k \neq i}}^{n} \frac{X - x_k}{x_i - x_k} = \sum_{i=1}^{n} \alpha_i \cdot L_i(X) \tag{3}$$

where n is a nonzero integer, $(x_i)_{1 \leqslant i \leqslant n}$ are collocation points, as roots of the Hermite polynomials available in [17], and $(\alpha_i)_{1 \leqslant i \leqslant n}$ are weights associated with Lagrange polynomials $(L_i)_{1 \leqslant i \leqslant n}$. It then becomes possible to express the following identification:

$$\forall i \in \{1; n\} \alpha_i = g(x_i) \tag{4}$$

By substituting (4) into (3), the r.v. Z is approximated by the r.v. $\tilde{Z}$, such that:

$$\tilde{Z} = \tilde{g}(X) = \sum_{i=1}^{n} g(x_i) \cdot L_i(X) \tag{5}$$

3. The j-order moment of r.v. Z that models the mechanical response is written as:

$$\mu_{j,Z} = \int_{-\infty}^{+\infty} g^j(t) \cdot p_X(t) \cdot dt \tag{6}$$

Using Eqs. (4)–(6), the mean of Z can then approximated by:

$$\mu_{1,Z} \approx \tilde{\mu}_Z = \sum_{i=1}^{n} p_X(x_i) \cdot g(x_i) = \sum_{i=1}^{n} \omega_i \cdot g(x_i) \tag{7}$$

where $(\omega_i)_{1 \leqslant i \leqslant n}$ are the weights associated with collocation points $(x_i)_{1 \leqslant i \leqslant n}$. The approximation $\tilde{\sigma}_Z$ of the standard deviation σ_Z of Z can then be expressed as:

$$\sigma_Z^2 \approx \tilde{\sigma}_Z^2 = \sum_{i=1}^{n} (g(x_i))^2 \cdot \omega_i - (\tilde{\mu}_Z)^2 \tag{8}$$

The skewness $\beta_{1,Z}$ and kurtosis $\beta_{2,Z}$ are respectively written as follows:

$$\beta_{1,Z} = \left(\frac{|\mu_{3,Z}|}{\sigma_Z^3}\right)^2; \quad \beta_{2,Z} = \left(\frac{\mu_{4,Z}}{\sigma_Z^4}\right)^2 \tag{9}$$

and approximated by:

Please cite this article in press as: Baroth J, Malecot Y. Probabilistic analysis of the inverse analysis of an excavation problem. Comput Geotech (2010), doi:10.1016/j.compgeo.2009.12.006

$$\tilde{\beta}_{1,Z} = \left(\frac{\left| \sum_{i=1}^{n} (g(x_i))^3 \cdot \omega_i \right|}{\tilde{\sigma}_Z^3} \right)^2; \quad \tilde{\beta}_{2,Z} = \left(\frac{\sum_{i=1}^{n} (g(x_i))^3 \cdot \omega_i}{\tilde{\sigma}_Z^4} \right)^2 \tag{10}$$

4. The PDF of r.v. Z, denoted p_Z, can then be approximated by the PDF $p_{\tilde{Z}}$ of r.v. $\tilde{Z}$, which is an analytical response surface (5). It is thus possible to obtain an estimation of the PDF using Monte Carlo simulations.
5. From PDF $p_{\tilde{Z}}$, an approximation of the η% confidence interval I_η, defined by:

$$z \in I_\eta \iff P(z \in I_\eta) \leqslant \frac{\eta}{100} \tag{11}$$

is evaluated using the confidence interval for the approximation $\tilde{Z}$ of r.v. Z, which can be written as:

$$\tilde{I}_\eta = [\tilde{z}^\eta_{\text{inf}}; \tilde{z}^\eta_{\text{sup}}] \iff \int_{\tilde{z}^\eta_{\text{inf}}}^{\tilde{z}^\eta_{\text{sup}}} p_{\tilde{Z}}(z) \cdot dz \leqslant \frac{\eta}{100} \tag{12}$$

Approximations of the bounds $\tilde{z}^\eta_{\text{inf}}$ and $\tilde{z}^\eta_{\text{sup}}$ can then be practically deduced from $p_{\tilde{Z}}$.

This SFEM greatly reduces the number of mechanical computations in comparison with Monte Carlo methods [20]. The methodology presented herein is of optimal use for an analysis with few input random variables and a time-consuming FE model, which is typical of nonlinear cases.

4. Application to an excavation problem

4.1. The genetic algorithm (GA) inverse analysis

The adopted finite element model (2D plane strain) is shown in Fig. 3 (see also the numerical details contained in Table 1). The symmetric excavation under analysis, which measures 6 m deep by 20 m wide, is supported by a sheet pile wall whose head is stabilised by a strut. Our focus lies on the horizontal wall displacements, which have been coalesced into vector z. Two successive loading steps have been set: at first, only the weight of the soil is considered (Phase 1), then a 30 kN loading is applied at a distance of 1 m from the head (A–A in Fig. 3). The soil is composed of a single layer of homogeneous sand modelled by a five-parameter Mohr–Coulomb model. The effect of water is limited to hydrostatic pressure. In order to decrease the number of uncertain parameters, we have assumed *a priori* values for parameters showing a weak influence within their possible variation range or for parameters whose values could be known from empirical relations: the cohesion c is considered equal to zero, Poisson's ratio ν equal to 0.25, and the dilatancy angle $\psi = \varphi - 30°$, where φ is the friction angle.

Table 1
Characteristics of the numerical excavation model.

Problem size: L = 50 m, H = 25 m
Excavation size: h = 6 m, l = 2 × 10 m
Wall height: h_w = 9 m
Plane strain, type of elements = triangles with 15 nodes
419 elements, 3695 nodes, 5028 stress points

Moreover, in assuming a normally-consolidated behaviour for the sand, we make use of the Jaky relation to determine the initial stress field (coefficient $K_0 = 1 - \sin\varphi$).

Taking everything into account, we first applied the identification method to determine two parameters: shear modulus G_{ref}, and friction angle φ, which are the only uncertain parameters examined in the analyses that follow.

4.1.1. Synthetic measurements

To test the method, the measurements consisted of numerical results from this simplified problem instead of using true experimental data. These first steps have allowed avoiding errors stemming from both the measurements and the numerical modelling.

We have arbitrarily set G_{ref} = 22,500 kPa and φ = 35° so as to numerically create an "experimental" wall displacement curve $u_x(z)$ (see Fig. 4). Horizontal displacements of the sheet pile wall u_x are obtained from nodal displacements of the wall at each depth z. From this point, G_{ref} and φ have been considered as uncertain parameters. Since this study is fully synthetic, we arbitrarily decided that a reasonable error associated with these measured displacements could be evaluated as $\Delta = \pm|0.5\text{ mm} + 3\%|$, where 0.5 mm represents the absolute part and 3% the relative part of measurements error. This error has been plotted on Fig. 4 in dashed lines. It is supposed to represent both the measurement error and the modelling approximation (geometry, constitutive law, heterogeneity...) which would occurred in a real case.

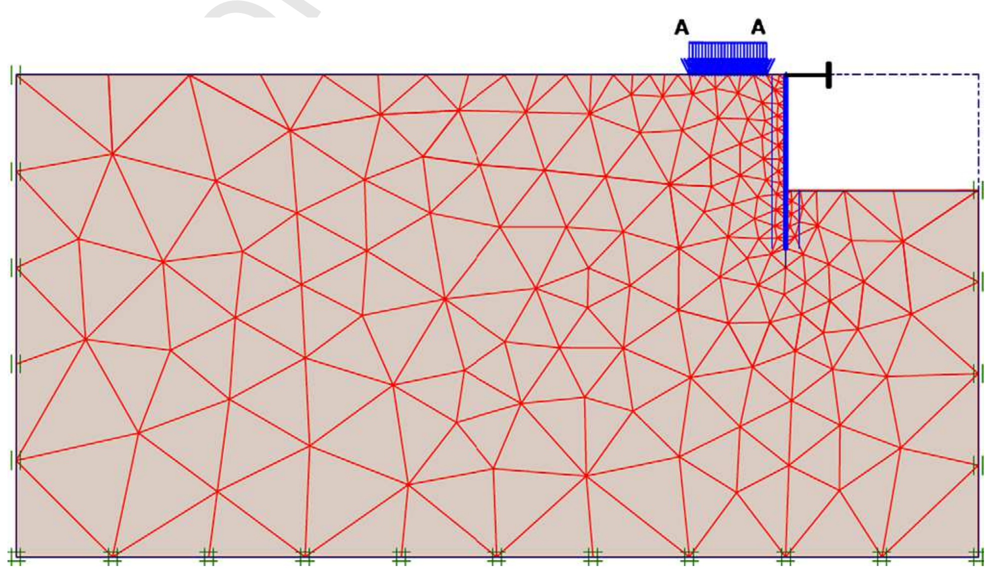

Fig. 3. Numerical excavation problem: 2D (plane strain) model and its associated mesh ($L \times H$ = 50 × 25 m, excavation size: h = 6 m, l = 2 × 10 m, wall height: h_w = 9 m, mesh: 419 FE).

Please cite this article in press as: Baroth J, Malecot Y. Probabilistic analysis of the inverse analysis of an excavation problem. Comput Geotech (2010), doi:10.1016/j.compgeo.2009.12.006

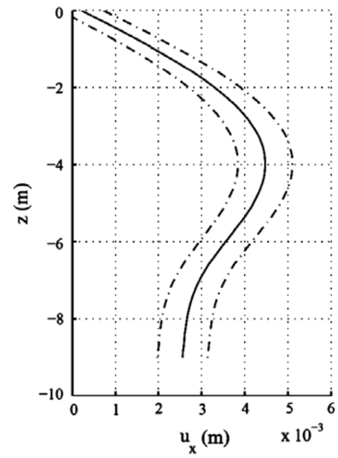

Fig. 4. Measured horizontal displacements of the diaphragm wall, versus depths (full line), and the corresponding tolerable margin for the response of the numerical model $\pm\Delta$ (dashed lines).

4.1.2. Statistical characterisation of G_{ref} and φ using the genetic algorithm

Table 2 presents the set of parameters obtained from the genetic algorithm identification method. Method results consist of a pool of 87 solutions, couples of shear modulus (in kPa) and friction angle (°) values, denoted (G_i, φ_i), $i = 1, \ldots, N = 20$ [15]. Since some couple values are equal, a total of $N_s = 20$ solutions were eventually identified; each identified solution was then associated with a frequency of occurrence. Estimations of means (m_φ, m_G) and standard deviations $(\sigma_\varphi, \sigma_G)$, as well as coefficients of variation $(Cv_\varphi = \sigma_\varphi/m_\varphi, Cv_G = \sigma_\varphi/m_\varphi)$ and correlation coefficient $\rho_{\varphi G}$, are listed in Table 3. The correlation coefficient between the friction angle and shear modulus ($\rho_{\varphi G} = -0.62$) is a result of the identification process. This correlation is specific to the numerical model and to the associated measurements. It is a consequence of the non-uniqueness of the solution of the inverse problem. In the present case, it describes a simple mechanical property of the wall displacements: for each couple (G_i, φ_i), a slight increase of the friction angle φ and decrease of the shear modulus G leads to the same displacement of the wall and vice versa.

Table 2
Parameters of the genetic algorithm identification method.

Number of uncertain parameters: $N_p = 2$
Size of the search space: 11,000 kPa < G_{ref} < 83,000 kPa, 14 < φ < 46°
Number of bits allocated to an individual: $N_b = 12$
Number of individuals in a population: $N_I = 120$
Number of crossing points for reproduction: $N_{coup} = 2$
Mutation ratio: $P_M = 3\%$
Tolerable error on the error function: $\delta F_{err} = 3\%$
Number of identified solutions: $N_s = 20$

Table 3
Estimations of means, covariance and correlation coefficients of identified parameters.

Friction angle mean: $m\varphi = 34.99°$
Coefficient of variation for the friction angle: $Cv\varphi = 2.86\%$
Shear modulus mean: $m_G = 22{,}857$ kPa
Coefficient of variation for the shear modulus: $Cv_G = 10.6\%$
Coefficient of correlation between friction angle and shear modulus: $\rho_{\varphi G} = -0.62$

4.2. Stochastic finite element method (SFEM) prediction

This section is intended to:

- characterise horizontal displacements of the diaphragm wall: statistical moments, probability density function (PDF) and confidence interval;
- verify that the assumptions adopted concerning uncertainty of the deformed diaphragm wall are indeed relevant; and
- predict horizontal displacements when a structure is built after excavation.

The probabilistic assumptions are proposed as a first step. The algorithm of the SFEM applied to the inverse analysis results is also presented. The SFEM is then calibrated by considering only the horizontal displacement prediction for one point of the deformed wall. The calibrated method is ultimately applied to various points on the wall.

4.2.1. Probabilistic assumptions

Two random variables (r.v.), denoted Y_1 and Y_2, are considered for the purpose of modelling the variability of both shear modulus G and friction angle φ.

From the previous section, empirical estimations of means m_G and $m\varphi$ are deduced based on 87 samples. In introducing the assumption of Gaussian distributions, 95% confidence intervals for these means are evaluated at ±1.3% and $\Delta \pm 0.4\%$, respectively. This estimation is generated from a sample size-dependent Student's t-distribution. Such uncertainty due to a limited number of data elements demonstrates the lack of a need to derive highly-precise probabilistic characteristics. Therefore, following probabilistic analyses will be restricted to the evaluation of second order characteristics (mean, coefficients of variation). Moreover, 95% confidence intervals seem also more relevant than 99% ones.

Y_1 and Y_2 are first assumed to be Gaussian, with means μ_{Y_1}, μ_{Y_2}, standard deviations $\sigma_{Y_1}, \sigma_{Y_2}$ and correlation coefficient $\rho_{Y_1Y_2}$, which are respectively equal to m_G, $m\varphi$, σ_G, $\sigma\varphi$ and $\rho_{G\varphi}$ (see Table 3).

4.2.2. SFEM algorithm

This section presents the algorithm of the stochastic approach applied to inverse analysis results, considering n integration points and the two random variables Y_1 and Y_2 [17].

- generate n quadrature points and weights (x_i, w_i), for $1 \leqslant i \leqslant n$ associated with the standard Gaussian law;
- generate n^2 couples of points $\boldsymbol{y} = (y_1^i, y_2^j)$ of $\boldsymbol{Y} = (Y_1, Y_2)$, such that $\boldsymbol{y} = T(\boldsymbol{x})$, where $\boldsymbol{x} = (x_i, x_j)$, for $1 \leqslant i,j \leqslant n$; characteristics of $\boldsymbol{Y}$, namely, $\mu_{Y_1}, \mu_{Y_2}, \sigma_{Y_1}, \sigma_{Y_2}, \rho_{Y_1Y_2}$ are deduced from the statistical analysis of the GA calculations;
- compute the n^2 outcomes $z^{ij} = z(y_1^i, y_2^j)$, for $1 \leqslant i,j \leqslant n$, given by the FE model;
- the numerical solution writes

$$z \approx \tilde{z}(y_1, y_2) = \sum_{i=1}^{n} \sum_{j=1}^{n} z^{ij} L_i(y_1) L_j(y_2) \tag{13}$$

where L_i, L_j are Lagrange polynomials from (3).

- the mean and standard deviation of the approximate stochastic solution $\tilde{Z}$ are

$$\mu_{\tilde{Z}} = \sum_{i=1}^{n} \sum_{j=1}^{n} z^{ij} \omega_i \omega_j \quad \text{and} \quad \sigma_{\tilde{Z}}^2 = \sum_{i=1}^{n} \sum_{j=1}^{n} (z^{ij})^2 \omega_i \omega_j - \mu_{\tilde{Z}}^2.$$

Please cite this article in press as: Baroth J, Malecot Y. Probabilistic analysis of the inverse analysis of an excavation problem. Comput Geotech (2010), doi:10.1016/j.compgeo.2009.12.006

Table 4
Evolution of the statistical moments of r.v. Z for various numbers of integration points.

Number of integration points	$\tilde{\mu}_Z$ (mm)	$\tilde{\sigma}_Z$ (mm)	$\tilde{\beta}_{1,Z}$	$\tilde{\beta}_{2,Z}$
3 × 3	4.34	0.388	0.304	2.47
4 × 4	4.394	0.3421	0.369	3.23
5 × 5	4.392	0.3416	0.385	3.19

- the probability density function can be estimated from (13) by using a Monte Carlo approach.

4.2.3. SFEM calibration

This section will focus exclusively on the horizontal displacement prediction for one point of the deformed diaphragm wall (−4.5 m, see Fig. 4). The displacement is modelled using a scalar r.v. Z, which has to be characterised by coefficients of variation and confidence intervals for different depths.

Table 4 displays the evolution of statistical moments of r.v. Z, for $n = 3 \times 3$, 4×4 and 5×5 integration points. For both 4 and 5 integration points per r.v., the mean and standard deviation of Z are nearly equal to: $\mu_Z = 4.4$ mm and $\sigma_Z = 0.3$ mm. For both 4 and 5 integration points per r.v., the skewness and kurtosis of Z almost equal $\beta_{1,Z} = 0.4$ and $\beta_{2,Z} = 3.2$. These adimensional coefficients describe the shape of the PDF of Z, which is plotted in Fig. 5 for $n = 3$, 4 and 5; this figure reveals that the curves for $n = 4$ and 5 are very similar, which is why additional integration points are not considered necessary in the present work. More detailed studies of numerical convergence are available in [17,22,23,27], where $n = 4$ was found to offer a good compromise between computational effort and accuracy.

$N = 100{,}000$ samples are used in Fig. 5 to represent the PDF of r.v. Z. In order to evaluate the effect of N, various PDFs have been plotted in Fig. 6, for $N = 10^3$, 10^4 and 10^5 samples, with $n = 4$ integration points.

Since 10^5 samples are required to obtain a relatively smooth PDF, 10^4 samples prove sufficient to determine the 95% confidence interval on the studied displacement (see Table 5).

Whilst the Gaussian assumption leads to an estimation of uncertainty regarding data, it suffers from the limitation that the normal distribution is not representative of real data for the shear modulus and friction angle (which are always positive) and, for this reason, lognormal PDFs for the input random variables will be considered in the following discussion.

Table 6 presents approximated statistical moments and the 95% confidence interval $\tilde{I}_{95\%}$ for r.v. Z with $n = 4$ integration points, for both Gaussian and lognormal random variables Y_1 and Y_2. Since the means, standard deviations and kurtosis are all quite close to one another, skewness and the 95% confidence interval are logically quite different. Nevertheless, Fig. 7 shows that the resulting PDFs remain close, even if values of skewness are quite different. The r.v. Z does not seem to greatly depend on the distribution type of input random variables. After this study, the lognormal law has been chosen to represent input random variables Y_1 and Y_2.

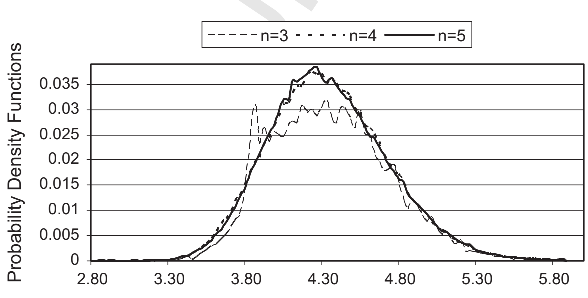

Fig. 5. Probability density functions (PDFs) of random variable Z (wall displacement at −4.5 m); Y_1 and Y_2 Gaussian; $N = 100{,}000$ samples; $n = 3$, 4 and 5.

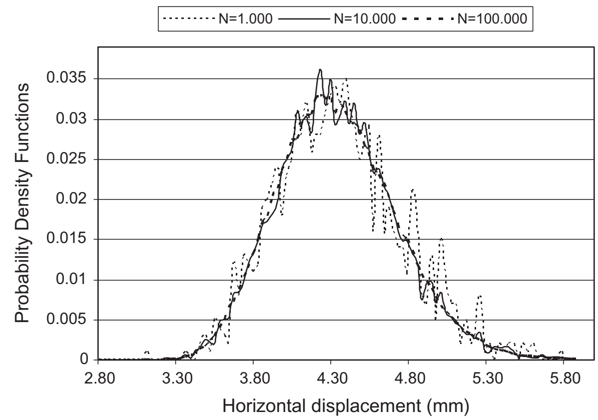

Fig. 6. Probability density functions (PDFs) of random variable Z for various numbers N of samples ($n = 4$ integration points), $N = 10^3$, 10^4 and 10^5.

Table 5
Evolution of the 95% confidence interval of r.v. Z, with $n = 4$ integration points, for a Gaussian distribution of input r.v.

Number of samples	$\tilde{I}_{95\%}$ (mm)
1000	3.3–5.2
5000	3.4–5.1
10,000	3.4–5.1
20,000	3.4–5.1
100,000	3.4–5.1

Table 6
Evolution of the statistical moments and 95% confidence interval of random variable Z (sheet pile displacement at −4.5 m) – $n = 4$ integration points.

Distribution law	$\tilde{\mu}_Z$ (mm)	$\tilde{\sigma}_Z$ (mm)	$\tilde{\beta}_{1,Z}$	$\tilde{\beta}_{2,Z}$	$\tilde{I}_{95\%}$ (mm)
Gaussian	4.39	0.342	3.7	3.2	3.5–4.98
Lognormal	4.39	0.351	1.2	3.3	3.2–4.99

4.2.4. Application of the calibrated method to various points of the wall

Fig. 8 shows the evolution of mean horizontal displacements and boundaries of the 95% confidence intervals for various wall depths. Confidence intervals have been deduced from 10,000 samples. This figure also compares the inverse analysis (IA) method assumption ($\Delta = \pm|0.5$ mm + 3%|, see Section 4.1.1) with SFEM evaluations of 95% confidence intervals. Just one SFEM confidence interval boundary lies outside the IA confidence intervals. Therefore, the SFE prediction allow to verify that the IA assumption do seem relevant.

4.2.5. Prediction of displacements during Phase 2

Table 7 lists the approximated statistical moments of the r.v. Z with $n = 4$ integration points for the lognormal random variables Y_1 and Y_2. During Phases 1 and 2, the coefficients of variation of Z range between 6% and 11% and between 7% and 14%, respectively, and they are higher at the base of the wall. These results show the effect of the variability of the shear modulus and of the friction angle on the variability of displacements. Indeed, Table 7 means that

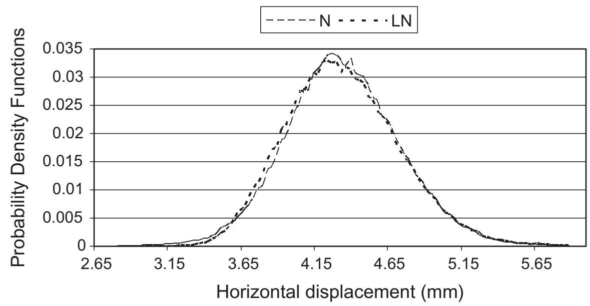

Fig. 7. Probability density functions of Z for Gaussian and lognormal random variables Y_1 and Y_2 (depth: −4.5 m); $n = 4$ integration points; $N = 100{,}000$ samples.

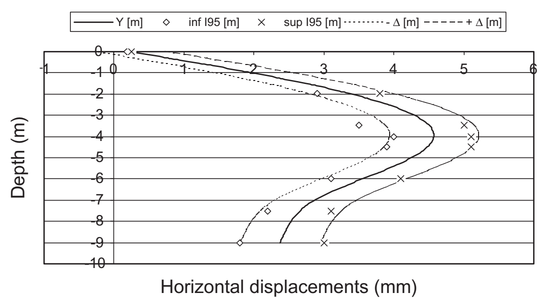

Fig. 8. Mean horizontal displacements and boundaries of the inverse analysis and SFEM 95% confidence intervals, for various wall depths (Phase 1); inf I95 and sup I95 denote boundaries of intervals, for each depth.

Table 7
Coefficients of variation for displacement modelling with r.v. Z ($n = 4$).

Depth (m)	Cov. (%) Phase 1	Cov. (%) Phase 2
0	7.6	7.8
−2	7.8	8.7
−3.5	7.4	8.8
−4	6.5	8.8
−4.5	6.4	8.8
−6	6.5	8.4
−7.5	8.7	7.6
−9	11.5	14.4

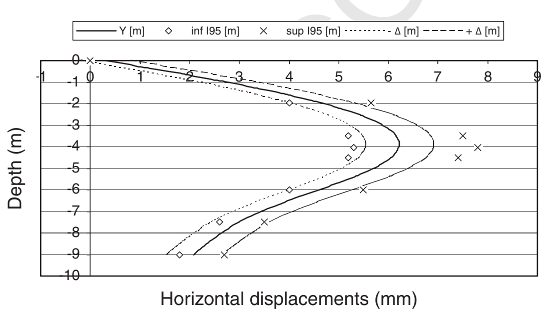

Fig. 9. Mean horizontal displacements and boundaries of inverse analysis and SFEM 95% confidence intervals, for various wall depths (Phase 2); inf I95 and sup I95 denote boundaries of intervals, for each depth.

the increases of square deviations of these displacements are greater than the increases of their means. This nonlinear effect illustrates how crucial it is to take into account soil properties variability.

Fig. 9 presents the mean horizontal displacements and 95% confidence interval boundaries (SFEM) for various wall depths. IA confidence interval boundaries ($\Delta = \pm|0.5$ mm + 3%|) are also plotted. It can be observed that many SFEM 95% confidence interval boundaries lie outside the IA confidence intervals in Phase 2. Reminding that SFEM 95% confidence interval boundaries were inside IA confidence intervals in Phase 1, the nonlinearity the mechanical problem is illustrated once again. It underscores that predicting only mean values of displacements is not secure. It finally quantifies the variability of the mechanical response by the estimation of confidence intervals of final diaphragm wall displacements.

5. Conclusion

This paper has discussed the combination of an inverse analysis technique based on a genetic algorithm with a stochastic finite element method, with the aim of improving the design of geotechnical structures through introducing a stochastic context. A genetic algorithm inverse analysis was first carried out to determine soil parameters from *in situ* measurements. The soil layers studies in this paper are assumed to be homogeneous and spatial variability, where the properties vary from one location (or finite element) to another, is not explicitly treated. These statistically-identified parameters were then used as input data to a stochastic finite element method. The second analysis allowed predicting a confidence interval for the final behaviour of the geotechnical structure. The tools employed in this study have already been presented in previous papers, but the originality herein consists of coupling them.

A FE code applied the method to estimate horizontal displacements of the diaphragm wall used in the synthetic excavation problem. This simple application case indicates that for a given tolerable error between the measurement and the response of the numerical model during the excavation process, the method leads to predicting a confidence interval for the final wall displacements.

The presented approach has to be suited to describe a heterogeneous soil. In case that different soil layers can be considered, authors think reasonable to apply these tools. In case of a strongly heterogeneous soil, the method has to be improved. Indeed, the statistical treatment of measurements has to be completed by the evaluation of a variogram and the corresponding correlation length. This information can be deduced if additional trial holes are managed, which is sometimes nonpracticable and always expensive. Then the probabilistic has to model the identified parameters by correlated random fields, for example using high-dimensional integration formulas [27] or Karhunen-Loève expansions [18].

In case the homogeneity of the studied soil layer can be assumed, future work will enable applying the method to real application cases and then extending it to reliability studies. It is for this reason that the proposed approach is likely to improve observational analysis methods for the design of geotechnical structures as part of the framework adopted in national and international building codes.

References

[1] Terzaghi K, Peck RB. Mécanique des sols appliquée aux travaux publics et aux bâtiment. Dunod 1957.
[2] Peck RB. Advantages and limitations of the observational method in applied soil mechanics. Géotechnique 1969;19(2):171–87.
[3] CEN. Eurocode 7 geotechnical design – part 1: general rules, prEN 1997-1; 2004.
[4] Tarantola A. Inverse problem theory: methods for data fitting and model parameter estimation. Elsevier Science B.V; 1987.
[5] Gioda G, Sakurai S. Back analysis procedures for the interpretation of field measurements in geomechanics. Int J Numer Anal Methods Geomech 1987;11:555–83.

[6] Ledesma A, Gens A, Alonso EE. Estimation of parameters in geotechnical backanalysis – 1. Maximum likelihood approach. Comput Geotech 1996;18(1):1–27.
[7] Anandarajah A, Agarwal D. Computer-aides calibration of soil plasticity model. Int J Numer Anal Methods Geomech 1991;15:835–56.
[8] Gens A, Ledesma A, Alonso EE. Estimation of parameters in geotechnical backanalysis – 2. Application to a tunnel excavation problem. Comput Geotech 1996;18(1):29–46.
[9] Zentar R, Hicher PY, Moulin G. Identification of soil parameters by inverse analysis. Comput Geotech 2001;28:129–44.
[10] Lecampion B, Contantinescu A, Nguyen Minh D. Parameter identification for lined tunnels in viscoplastic medium. Int J Numer Anal Methods Geomech 2002;26:191–211.
[11] Calvello M, Finno RJ. Selecting parameters to optimize in model calibration by inverse analysis. Comput Geotech 2004;31:411–25.
[12] Lecampion B, Contantinescu A. Sensitivity analysis for parameter identification in quasi-static poroelasticity. Int J Numer Anal Methods Geomech 2005;29:163–85.
[13] Finno RJ, Calvello M. Supported excavations: observational method and inverse modeling. J Geotech Geoenviron Eng 2005;131(7):826–36.
[14] Levasseur S, Malecot Y, Boulon M, Flavigny E. Soil parameter identification using a genetic algorithm. Int J Numer Anal Methods Geomech 2008;32(2):189–213.
[15] Levasseur S, Malecot Y, Boulon M, Flavigny E. Statistical inverse analysis based on genetic algorithm and principal component analysis: method and developments using synthetic data. Int J Numer Anal Methods Geomech 2009;33(12):1485–511.
[16] Levasseur S, Malecot Y, Boulon M, Flavigny E. Statistical inverse analysis based on genetic algorithm and principal component analysis: applications to excavation problems and pressuremeter tests. Int J Numer Anal Methods Geomech 2009. doi:10.1002/nag.81.
[17] Baroth J, Chauvière C, Bressolette P, Fogli M. An efficient SFE method using Lagrange polynomials: application to nonlinear mechanical problems with uncertain parameters. Comput Meth Appl Mech Eng 2007;196:4419–29.
[18] Matthies HG, Brenner CE, Bucher CG, Guedes Soares C. Uncertainties in probabilistic numerical analysis of structures and solids – stochastic finite elements. Struct Safety 1997;19(3):283–336.
[19] Lemaire M. Structural reliability. ISTE Publishing Company; 2008.
[20] Shreider YA. The Monte-Carlo method. Pergamon Press; 1966.
[21] Humbert J, Baroth J, Daudeville L. Probabilistic analysis of a pull-out test. Mater Struct, preprint; 2009.
[22] Rhayma N, Bressolette P, Baroth J, Boucha A. SFE analysis of a steel connection component. In: Proceedings of the tenth international conference on applications of statistics and probability (ICASP10), Tokyo, Japan; 2007.
[23] Goldberg DE. Algorithmes génétiques: exploration, optimisation et apprentissage automatique. Ed. Adisson-Weslety; 1991.
[24] Rechea BC, Levasseur S, Finno RJ. Inverse analysis techniques for parameter identification in simulation of excavation support systems. Comput Geotech 2008;35(3):331–45.
[25] Renders JM. Algorithmes génétiques et réseaux de neurones. Hermès; 1994.
[26] Pal S, Wathugala GW, Kundu S. Calibration of a constitutive model using genetic algorithms. Comput Geotech 1996;19(4).
[27] Bressolette P, Chauvière C, Baroth J, Fogli M. High-dimensional integration formulas for efficient SFE methods. In: Proceedings of the tenth international conference on applications of statistics and probability (ICASP10), Tokyo, Japan; 2007.

Please cite this article in press as: Baroth J, Malecot Y. Probabilistic analysis of the inverse analysis of an excavation problem. Comput Geotech (2010), doi:10.1016/j.compgeo.2009.12.006